Analysis of lunar crater timings, 1842–2011

David Herald & Roger W. Sinnott

Crater timings are made during a total or partial lunar eclipse as the Moon slowly glides through the Earth's central shadow cone, or umbra. We have gathered 22,539 observations made at 94 lunar eclipses since 1842 – the largest collection of crater and contact timings ever compiled. In this paper we analyse these timings to derive an improved characterisation of the umbra's size, shape, and stability over time.

Introduction

Crater timings are made during total or partial lunar eclipses. The moment when either the rim or the midpoint of a lunar feature (usually a crater) coincides with the umbra's edge is recorded. This edge, while somewhat diffuse, is well enough defined for timings by different observers to agree to better than one minute.

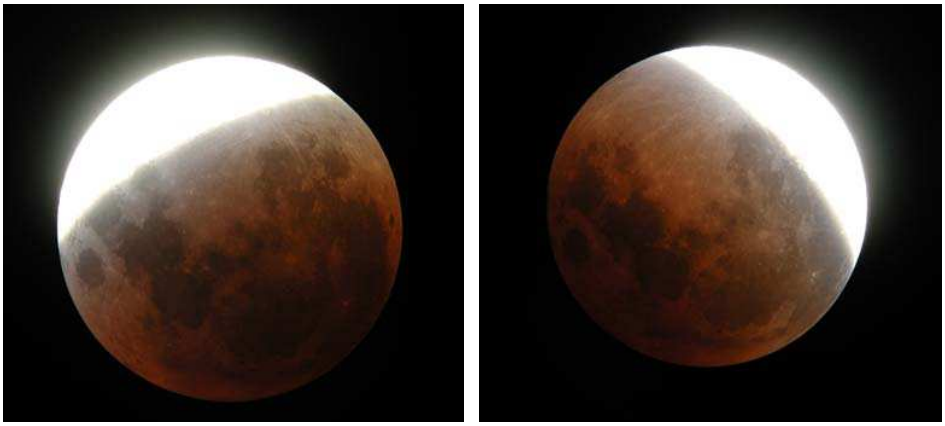

The umbra's edge photographed by Dennis di Cicco at the lunar eclipse of 2003 November 8.

The apparent ease with which the umbra's edge can be located has made crater timings attractive for observers since the early years of the telescope, when eclipse predictions were not reliable and the selenographic coordinates of craters poorly known. For example, during a 1736 eclipse George Graham & James Short, using a 5½-inch reflector magnifying 38 times, recorded the moment the umbra reached the east sides of Tycho, Plato, Manilius, and Mare Crisium to the nearest 5 seconds. John Bevis observed the same eclipse with a 5-foot telescope and noted when the umbra first touched Grimaldi and, 175 seconds later, covered it.[1]

Since those early observations, numerous authors have drawn various conclusions about the size and shape of the umbra, and its stability over time – usually on the basis of a small number of eclipses.

In this paper we analyse 22,539 observations made at 94 lunar eclipses since 1842 to derive an improved characterisation of the umbra's size, shape, and stability over time.

Reduction methodology

As early as 1687 the French astronomer Philippe de la Hire, in his predictions of lunar eclipses, added 90 arcseconds to the umbra's geometric radius to take into account the extra silhouetting effect of the Earth's atmosphere.[2] Later he revised this angle to 60 arcseconds. In both cases, de la Hire treated the enlargement as a fixed angle, additive to the umbral radius and independent of variations in the Sun–Earth–Moon geometry from one eclipse to another. The final enlargement value adopted by de la Hire, 60 arcseconds, is about 1/41 of the umbral radius that would otherwise be predicted if the Earth were airless.

Chauvenet approach

Numerous values for the umbral enlargement, ranging typically from 1/40 to 1/65, are found in the literature of the 18th and 19th centuries.[3,4] William Chauvenet, in his influential 1863 textbook,[5] selected 1/50, or 2%, as representative of the best determinations, corresponding to an enlargement factor, E, of 1.02.

Chauvenet expressed the umbra's observed angular radius, r_u, as follows:

$$r_u = (0.998340\,\pi_{Moon} - s_{Sun} + \pi_{Sun})E \qquad [1]$$

where π_{Moon} and π_{Sun} are the equatorial horizontal parallaxes of the Moon and Sun, respectively, and s_{Sun} is the geocentric semidiameter of the Sun. The factor 0.998340 is the Earth's radius at 45° latitude, the equatorial radius being 1. The factor serves as an 'average' radius of the oblate Earth and allows the umbra to be regarded as circular.

Equation [1], with E set to 1.02, is still used today in the *Astronomical Almanac* for predicting the primary contacts of lunar eclipses.[6]

To analyse observations, one calculates an observed r_u for each contact or crater timing and rearranges equation [1] to solve for E.

Danjon approach

In 1951, André Danjon argued that Chauvenet was not strictly correct to apply an enlargement factor to the entire expression for the geometric radius.[7] Among other problems, it leads to an erroneous enlargement of the penumbra (whose outer edge,

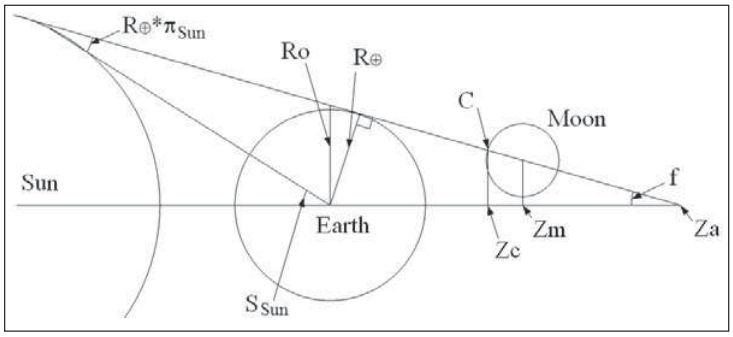

Figure 1. The geometry of a lunar eclipse. Here the Earth's radius, $R_\oplus$, is not a fixed quantity, because it includes the oblateness of the Earth's solid figure and also the notional eclipse-forming layer in the Earth's atmosphere.

admittedly, is not seen).

Instead, he regarded the Earth as increased in physical size by the atmosphere and applied this value to the lunar parallax alone, leading to the following expression:

$$r_u = (0.998340 + h)\,\pi_{Moon} - s_{Sun} + \pi_{Sun} \qquad [2]$$

where h is the effective height of the atmosphere for lunar eclipse purposes. An investigation of past eclipses led Danjon to estimate this height at 75 km, or 0.0118 Earth radii. The right side of equation [2] becomes very nearly $1.01\,\pi_{Moon} - s_{Sun} + \pi_{Sun}$, an expression used since 1951 in the *Connaissance des Temps* for predicting contacts of the Moon's limb with the umbra.

To analyse observations, one calculates an observed r_u for each contact or crater timing and rearranges equation [2] to solve for h.

Refined approach

Both Danjon and Chauvenet made simplifying assumptions:

- They treated the solid Earth as spherical (not oblate), with a radius equal to its true radius at 45° latitude;
- They considered the Moon to be located on the axis of the umbra, whereas timings are made when the Moon is between 0.5° and 1.0° from this axis;
- They made use of the Moon's parallax and its implied distance to the Moon's centre, but individual craters on the Moon's near side are slightly nearer the Earth and pass though a larger cross section of the umbral cone.

Thus, while equations [1] or [2] are convenient and useful approximations for predicting primary contact times, the analysis of crater timings requires a more detailed treatment.

We proceed in the spirit of Danjon's approach and derive, for each timing in the dataset, the corresponding height of a 'notional eclipse-forming layer' in the Earth's atmosphere (hereafter, the NEL height). Imagine a straight ray of light that extends from a point on the Sun's limb all the way to a particular point on the Moon's surface (or limb) that was timed as it entered or exited from the umbra. This straight ray grazes the Earth's atmosphere at a certain height above the solid surface. For entrances into the umbra, the ray represents the *last* possible ray of sunlight that could reach this lunar point. For exits from the umbra, it is the *first* such ray.

We do not suggest that the atmosphere literally blocks sunlight up to the heights (roughly 75 km) implied by crater timings. As early as 1936, Enzo Mora in Italy remarked that it is very difficult to believe that the atmosphere could significantly weaken the sunlight up to such heights.[8] It is merely a single quantity, derived from timings and free of the effect of the known oblateness of the solid Earth, that represents the effects of the Earth's atmosphere. Variations in NEL height from eclipse to eclipse would likely indicate changes in transparency and the scattering properties at lower atmospheric levels rather than atmospheric changes at the NEL height itself.

Figure 1 sets out the geometry of a lunar eclipse. The fundamental plane is that passing through the centre of the Earth and perpendicular to the umbral axis. The radius of the Earth (in equatorial Earth radii) at the tangent point of the shadow being $R_\oplus$, the half-angle, f, at the vertex of the shadow cone is given by $f = s_{Sun} - R_\oplus\,\pi_{Sun}$. The radius R_o of the umbral shadow on the fundamental plane is $R_\oplus$ / cos f, and the same radius through a crater at point C is as follows:

$$r_u = (R_\oplus / \cos f) - Z_c \tan f \qquad [3]$$

The distance Z_m of the Moon beyond the fundamental plane is obtained from the Besselian elements. The distance $(Z_m - Z_c)$ of a point on the Moon's surface at the edge of the shadow is obtained by projecting that point onto the plane through Z_m using the heliocentric lunar librations. Combining these gives the distance Z_c for use in [3]. Similarly that projection, when combined with the geocentric rectangular coordinates of the Moon, gives the location of the point on the Moon's surface relative to the shadow axis.

The value $R_\oplus$ is the effective radius of the Earth at some tangential point of the umbral shadow, and it includes the solid (oblate) Earth's radius plus the height of the NEL at that point. Having regard to the conical nature of this shadow, the relevant tangential latitude for the umbra's northernmost contact point with the Earth would be $90° - \delta_{Sun} - f$, where δ_{Sun} is the declination of the Sun. We may also define the position angle ψ for referring to various points around the edge of the umbra. By analogy with latitude on the Earth, ψ is measured northward (+) or southward (–) from the east-west direction on the sky.

As seen from the Sun, the Earth's apparent radius at angle ψ around the limb can be computed with sufficient accuracy as follows:

$$R_\oplus = 1 + h - 0.003353 \sin^2\psi \cos^2(\delta_{Sun} + f \sin\psi), \qquad [4]$$

where the constant 0.003353 is simply the Earth's flattening (usually expressed as 1/298.256). To analyse observations, one can:

- calculate the observed umbral radius r_u for each contact or crater timing,
- use [4], then [3], to calculate theoretical values of r_u corresponding to both $h = 0$ and $h = 0.02352$ Earth radii (that is, 150 km), and

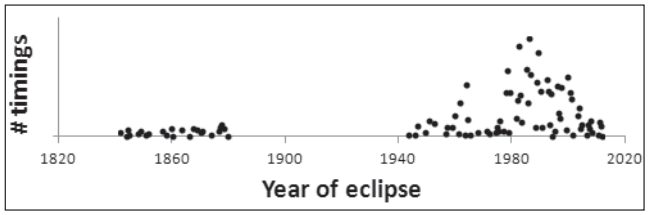

Figure 2. Relative number of crater timings by date. The dataset includes crater timings made over 170 years, with a 60-year gap in the middle.

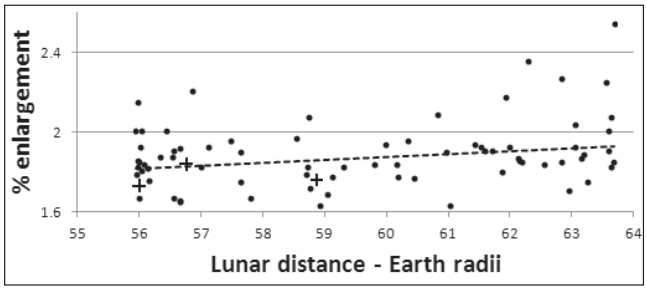

Figure 3a. The umbra's percentage enlargement (Chauvenet approach), plotted against lunar distance in Earth radii. Three particularly dark eclipses, indicated by crosses here and in Figure 3b, do not stand out from the rest.

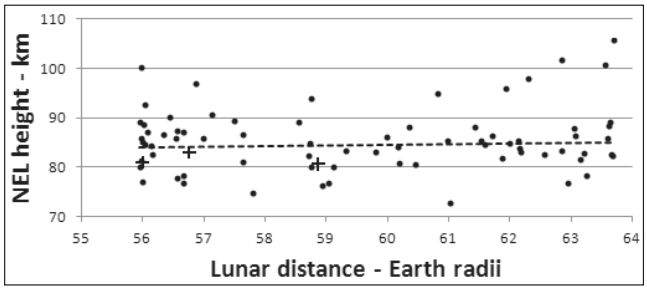

Figure 3b. The height of the notional eclipse-forming layer (Danjon approach), plotted against lunar distance.

- linearly interpolate the two theoretical values of r_u to match the observed radius, thereby obtaining the observed h value of the NEL.

Results

We have gathered 22,539 observations representing 26,685 individual timings at 94 lunar eclipses between 1842 and 2011. This is the largest collection of such timings ever assembled. We have archived the observations with the VizieR *Service for Astronomical Catalogues*, hosted by the Strasbourg astronomical data centre at **http://vizier.u-strasbg.fr/viz-bin/VizieR**. Our dataset is available as catalogue VI/140, and the associated *ReadMe* file contains details of sources. For example, it names the 764 individuals or groups who made the timings, and lists the 504 lunar features they observed. All the timings were made visually at the eyepiece, typically with telescopes of 5 to 25 cm aperture.

Figure 2 shows the number of observations by the date of the eclipse. While the dataset extends for almost 170 years, the number of observations made between 1960 and 2000 is far greater than in other epochs. This is the result of the observing programmes run by the late Byron Soulsby and also by *Sky & Telescope* magazine, initially under the late Joseph Ashbrook.

The online dataset includes the percentage enlargement as well as the height of the NEL, so that the data can be readily compared with previous results expressed as a percentage enlargement of the umbra.

The standard deviation of an individual timing is of the order of 25 to 30 secs. Most reports list the timings of specific observers separately, but a few provide, for each crater and event type, only a combined (average) time from several observers. In all cases, the dataset lists the number of observers associated with each timing.

In the dataset, 6% of the timings are for umbral contacts with the Moon's limb. Another 3% are for extended or irregular surface features such as maria and mountain ranges. Both kinds of timings show greater scatter than the rest. Accordingly, our discussion and plots (except where noted) are based solely on the 20,678 records, representing 24,264 individual timings, of craters and small spots on the lunar surface.

It is not our intention to model the physical causes of the umbral enlargement. Both Link[9] and Karkoschka[10] have made serious attempts to model the scattering and refractive effects of the Earth's atmosphere that give rise to the observed enlargement. Our results will help future modelling efforts.

Enlargement of the umbra

Figures 3a and 3b show the increased size of the umbra calculated by our algorithm as a function of the Moon's distance. The first plot shows the umbral enlargement as a percentage value (Chauvenet approach), while the second plot shows the NEL height in kilometers (Danjon approach).

As expected, the *percentage* enlargement depends somewhat on the lunar distance, but the NEL value does not. Thus it is *not* a good idea to consider 2% or any other fixed percentage as the typical umbral enlargement. It would be better to adopt a nominal NEL height and use that for predicting contact times and crater passages at future eclipses.

Nevertheless we derive 'best' values for both the percentage enlargement and the NEL height. As illustrated in Figures 4 and 5, the distribution of timings is slightly asymmetric – for reasons not yet understood. We therefore offer three standard statistical

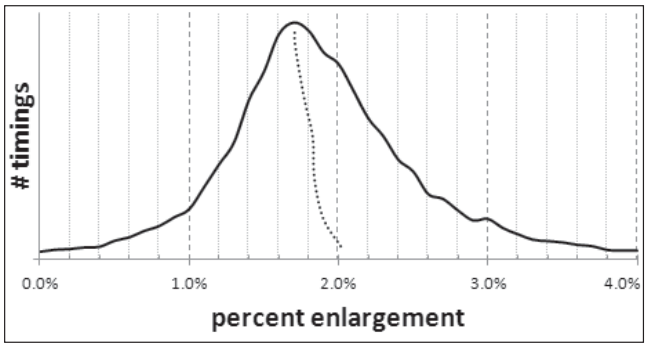

Figure 4. The distribution of percentage enlargement values in the dataset as a whole. Unlike a purely Gaussian distribution, this one is not quite symmetrical (as is emphasised by the dotted line, representing the midpoint at each level of the curve).

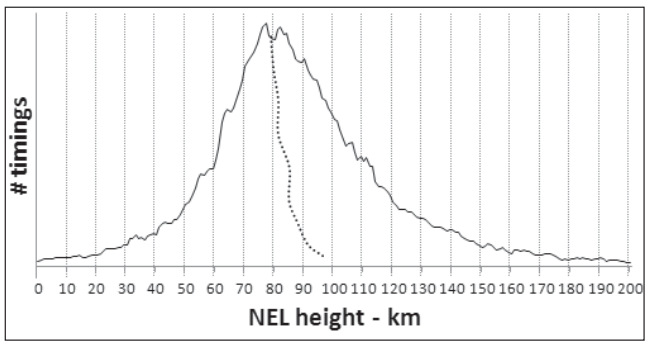

Figure 5. The distribution of NEL heights in the dataset also differs slightly from a Gaussian one. (This plot is more jagged than that for enlargement values because narrower 'bins' were used.)

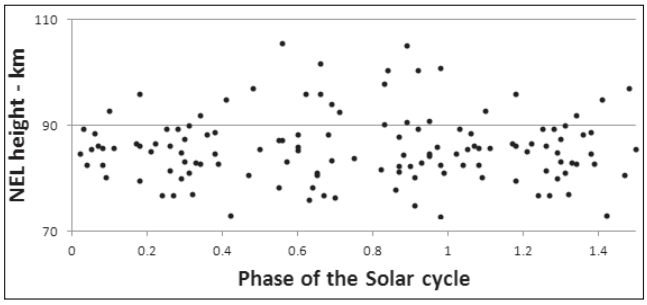

Figure 6. No clear periodicity is apparent when the NEL heights (one dot per eclipse) are plotted against their phase in the 11.2-year solar cycle.

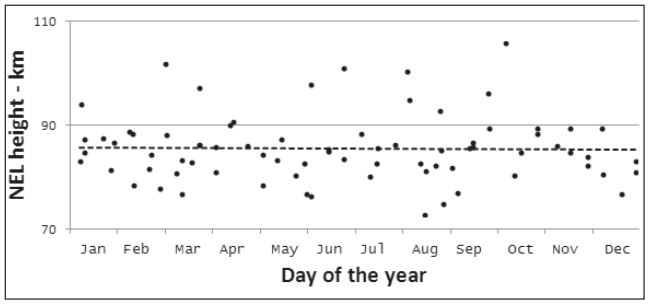

Figure 7. The distribution of NEL heights versus day of year also shows no clear features that could be associated with certain meteor showers or with seasonal changes in the atmosphere.

measures of the 'best' value for the percent enlargement and the NEL height.

For the percentage enlargement, the *modal* value (that encountered most often in the dataset) is 1.7%. The *median* value (for which the number of values smaller equals the number of values greater) is 1.8%. Finally, the *mean* enlargement is 1.88%.

For the NEL height, the *modal* value is 78 km, and the *median* is 85 km. The *mean* is 86.9 ± 0.2 km, where the quoted uncertainty is the standard deviation of the mean.

In summary, our derived enlargement percentages are all significantly smaller than the 2.0% Chauvenet value. Conversely our derived NEL heights are all larger than the 75 km of Danjon.

Cyclical variations in enlargement

During the 20th century the focus of most investigators shifted from finding a 'best' value for the umbral enlargement to studying the differences that occur from eclipse to eclipse, not only in the amount of umbral enlargement but also in the brightness and colour of the Moon during totality – and the possible causes and correlations among these differences.

Thus in 1921 Danjon studied 150 eclipses and reported that the brightness of a lunar eclipse appeared related to its placement in the 11-year solar activity cycle.[11] In the same paper he proposed his well-known five-point scale (0 through 4) by which future eclipses could be ranked by brightness and colour. These are commonly called *L* ratings.

However a 1950 analysis of 33 eclipses by Bouška & Švestka found only a weak correlation, at best, with solar activity.[12] They found even less correlation with the declinations of the Sun and Moon, or with the Earth–Sun and Earth–Moon distances. Instead, they mentioned meteoritic dust in the upper atmosphere as a possible factor, suggesting that increased particle levels in the days or weeks following annual meteor showers might yield a slightly swollen umbra. This idea gained further support in an analysis of 57 eclipses by Link & Linkova.[13]

Seasonal changes in atmospheric structure have also been proposed as possibly influencing the size of the umbra.[7]

Figures 6 and 7 plot the NEL height against the phase of the solar cycle and of the seasonal cycle, respectively. Neither plot shows any signs of a cyclical trend. We have also tested the data by the discrete Fourier transform (DFT) method, as implemented by Belserene to search for periodicities in the lightcurves of newly discovered variable stars.[14] The DFT analysis shows no hint of a period in the vicinity of either 1 year or 11 years.

We also checked for the existence of any long-period cyclic variation or secular trend in the NEL height. Figure 8 compares the observations made in the middle of the 19th century with those made in the latter part of the 20th century. The group of eclipses between 1949 and 1974 stands out, as the height often climbs well above 90 km for these eclipses. But the reports of those eclipses showed they were sparsely observed, and the observations were affected by cloudiness or the approach of moonset (implying interference by twilight). Thus we consider that the higher NEL heights from those eclipses are most likely spurious.

When those eclipses are disregarded, Figure 8 shows that there is no obvious long-term trend in the NEL height over 170 years, despite the major changes in human activity over this time period.

Incidental variations in umbral size

Major volcanic eruptions can lead to unusually dark lunar eclipses, owing to the vast quantities of aerosols spewed into the Earth's upper atmosphere. Keen[15] and Hofmann *et al.*[16] have investigated this connection in detail.

A particular example is the 1963 Dec 30 eclipse, where the unusual darkness was likely caused by the massive eruption, nine months earlier, of Mount Agung on Bali.[17] The eclipsed Moon's visual magnitude was only +4.1, as derived from 13 independent estimates at mid-totality collected by *Sky & Telescope*.[18] When Ashbrook analysed 600 crater timings from this eclipse he found the umbral enlargement to be nothing out of the ordinary.[19] Our own analysis concurs, with a mean NEL height of 87.1±1.4 km, compared to 86.9 km for the entire dataset.

We have not pursued further the direct relationship, if any, between eclipse brightness and NEL height. Reliable umbral brightnesses are hard to come by, especially for partial eclipses. Also, published Danjon *L* ratings show a great deal of scatter.

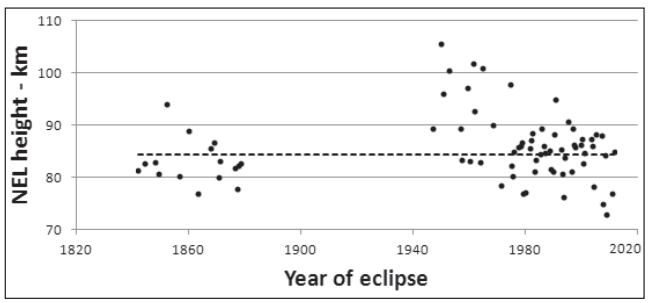

Figure 8. When a few poorly observed eclipses between 1943 and 1974 are ignored (see text), the NEL heights show no clear long-term trend from 1842 to 2011.

However the well-observed 1963 Dec 30 eclipse strongly suggests the absence of a correlation between eclipse brightness and the height of the NEL. (This eclipse, and those of 1982 Dec 30 and 1992 Dec 9, are indicated by crosses in Figures 3a and 3b.)

Other incidental variations in NEL height from one eclipse to another are amply confirmed by our data. The 1,164 timings of the 1982 July 6 eclipse yield a height of 90.7±1.2 km. The 1,119 timings of the 1989 Aug 17 eclipse give a height of 82.2±1.0 km. Changes in weather conditions around the Earth's terminator from eclipse to eclipse are likely responsible, but a specific cause has yet to be identified.

Oblateness of the umbra

The shape of the base of the umbral shadow cone (at the fundamental plane) is defined by the Earth's profile as seen from the Sun. The Earth is a flattened sphere. Furthermore, when an eclipse occurs near a solstice the apparent polar radius of the Earth is greater than when an eclipse occurs near an equinox – due to the different tilts of the Earth's polar axis towards the Sun. As a result the flattening of the base of the umbral shadow varies between about 1/298 for eclipses near an equinox, to about 1/355 for eclipses near a solstice.

As the shadow cone converges toward the Moon, the flattening in its cross section increases for purely geometrical reasons. In 1969 Ahnert & Meeus noted that the flattening of the umbra at the distance of the Moon is expected to be about 1/214 on average.[20]

However, various investigators have claimed the shape of the umbra to be different from that expected geometrically. An increased flattening was suggested in 1940 by Kosik[21] and affirmed in 1950 by Bouška, who wrote, 'It is evident that the true flattening of the shadow is much greater than the calculated one, corresponding to the Earth's flattening'.[22] Similar conclusions were reached by Link[9] and Ashbrook.[19] Schilling subsequently suggested that the height of the Earth's mesosphere may vary with latitude.[23] Ahnert & Meeus noted that the umbra's observed flattening could be accounted for if the troposphere were 10 km higher at the equator than at the poles.[20] Investigation of the umbra's increased flattening became a special passion of Soulsby.[24–27]

In our analysis we avoid any direct determination of the shape of the umbra. Rather, we use the observations to determine the NEL height above the oblate Earth's surface, so that any abnormal shape of the umbra will appear as a latitude-dependent variation of this height.

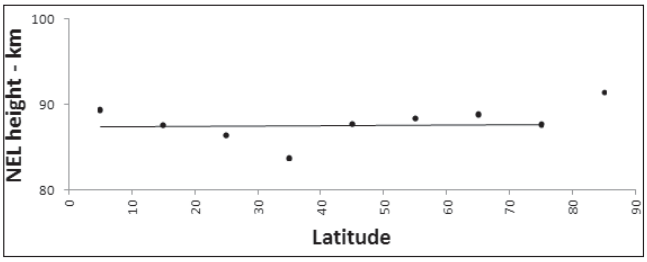

Figure 9. The NEL heights in the dataset are here grouped in 10° bins of angular position around the umbra (measured north or south of the east–west line, ignoring sign). Since there is no clear trend, we conclude the NEL height does not vary for sunlight grazing different latitudes on the Earth.

Figure 9 plots the average NEL height as a function of the angle ψ of each crater's contact point around the umbra measured from the east–west line (akin to latitude). For eclipses that occur near an equinox, ψ corresponds precisely with the geographic latitude of the NEL. For eclipses near the solstices this correspondence is still a fair approximation, except that near latitude 90° north or south the inclination of the pole towards or away from the Moon comes into play. (At a solstice, ψ value +90° or –90° implies tangency to the Earth at latitude +67° or –67, and observations cannot tell anything about the NEL at polar latitudes.)

The straight line in Figure 9 is a linear regression to the data points – excluding the point for 85° latitude (which had far fewer observations than any other latitude). Any abnormal increase in flattening would appear as a decrease in NEL height with increasing latitude. The absence of any such trend demonstrates that the shape of the umbral shadow is fully attributable to the oblateness of the Earth. Past conclusions that the observed flattening of the umbral shadow was greater than expected from the shape of the Earth are not supported by our analysis.

Differences between sunrise and sunset terminators

Bouška found that the umbral enlargement of the western part of the shadow for the 1957 May 13 lunar eclipse was 1/64, while that of the eastern part of the shadow was 1/50. He commented, 'The difference between both values may be explained by different meteorological conditions along the west and the east parts of the

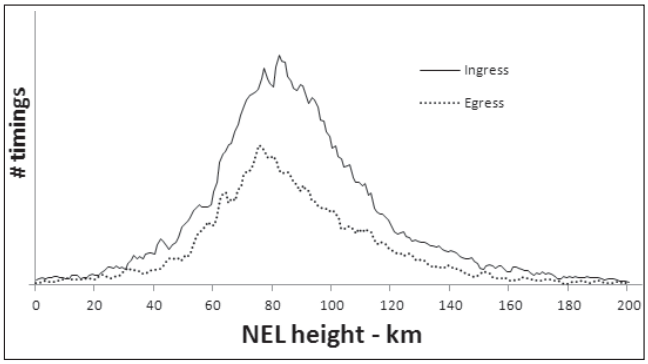

Figure 10. A comparison of height distributions for ingress and egress events.

Earth's terminator (high clouds)'.[28] However, he found no such difference for the 1959 Mar 24 eclipse.[29] In 1990 Soulsby analysed crater ingresses separately from egresses, using his own much larger collection of timings. While significant differences occurred for certain eclipses, Soulsby found that on average the enlargement was the same.[26]

In Figure 10 we compare the NEL height for ingress and egress separately. Our mean height is higher by 3.5 km for ingresses than for egresses.

Since crater ingresses serve as a probe of the sunset terminator of Earth, and egresses the sunrise terminator, it is *possible* that the difference has something to do with the transparency of the Earth's atmosphere at these two times of day. On the other hand, observational bias could be involved (see next section).

We consider the difference in height of 3.5 km between ingresses

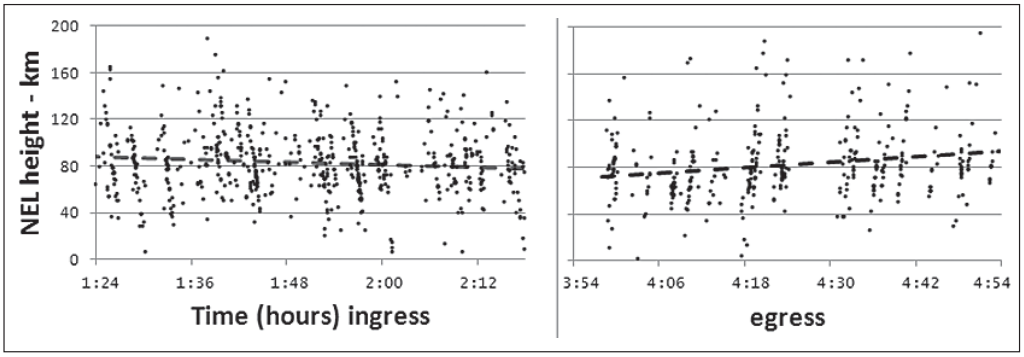

Figure 11. NEL heights found for limb contacts and individual craters during the well-observed eclipse of 1989 Aug 17. The left plot is for ingress, the right for egress, and the horizontal scales show Universal Time. Totality lasted from 2:20 to 3:56 UT. Note the tendency for heights to come out slightly smaller when the Moon as a whole is darkest (nearer totality), probably biasing observers' judgment of the umbral edge.

and egresses is insufficient to support a predictable, systematic difference in atmospheric transparency at the sunset and sunrise terminators. This is illustrated by two well-observed eclipses. At the 1986 Apr 24 eclipse, the height for the egresses was 10.2 km *higher* than for ingresses, whereas at the 1993 Nov 29 eclipse the height for the egresses was 15.4 km *lower* than for ingresses.

Bias in the timings

To make a timing, the observer must judge the location of the shadow edge. Articles soliciting timings have typically defined this edge as the point on the umbra–penumbra boundary where the change in light intensity is the greatest. When the timing involves a crater, the observer is able to compare the Moon's surface brightness on either side of the nominal edge, but this is not the case for primary contacts with the lunar limb. At first and fourth contact, the observer sees only the penumbral side of the umbra's edge. At second and third contact, the observer sees only the umbral side. Under these circumstances, reliable timing of primary contacts is, at best, a severe challenge.

Our dataset amply confirms the superior accuracy of crater timings over primary contact timings. There are many combinations of event types that might be compared, but a single example will make the point. In the entire dataset, craters and spots yield a mean NEL height of 88.2 km at ingress and 84.7 km at egress (not much difference). But for primary contacts it is 80.0 km and 90.4 km, respectively.

Even during the course of ingress and egress at a single, well-observed eclipse there can be subtle trends that suggest the perceived size of the umbra has some dependency upon how much of the Moon is in shadow, as illustrated in Figure 11. Another effect we have noted is the possibility that the height of the NEL is systematically affected by the observer's confidence in assessing the location of the edge of the umbra. However we leave these possible effects for future consideration, noting that from the dataset as a whole the height of the NEL is a well-determined 87 km.

An extreme contrarian view of bias at *all* lunar eclipses is included here for completeness. Marmet & Couture used laboratory simulations of a lunar eclipse to conclude that the umbral enlargement is purely an optical illusion that stems from the way the human eye and brain interpret the brightness gradient at the umbra's edge.[30]

If this were the case, the apparent angular extent of the umbral enlargement would be the same for all eclipses – independent of the lunar distance. This would require the physical extent of the umbral enlargement at the distance of the Moon to be greater when the Moon is further away, which in turn would require the observed height of the NEL to increase in proportion to the lunar distance. The required increase is of the order of 10 km over a change in the lunar distance of from 56 to 64 Earth radii. Figure 3b plots the observed height of the NEL against the lunar distance. The absence of any indication in Figure 3b of such a variation *prima facie* negates the hypothesis that the umbral enlargement is purely an optical illusion.

Conclusions

For the dataset as a whole, involving 20,000+ crater timings at 94 lunar eclipses over 170 years, we find no evidence for the cyclical variations or systematic anomalies in umbral size or shape that previous investigators have claimed. The size and shape of the umbra are consistent with the known shape and inclination of the solid Earth at the time of each eclipse, and with the concept of a notional eclipse-forming layer that envelopes the Earth uniformly. Any correlation with the brightness or darkness of the umbra is not statistically significant.

Our analysis confirms what has long been known, that the edge of the umbra is more reliably located using craters and spots than by contacts with the Moon's limb. The standard deviation of a single crater timing, even for an experienced observer, is no better than 25 to 30 seconds. This produces an uncertainty of about 25 to 30 km in NEL height (again, for a *single* timing), making it essential to combine many timings.

The size and consistency of the dataset suggest a way to improve predictions of future lunar eclipses. The traditional predictions using either the Chauvenet or Danjon approach include the simplification of a spherical Earth having a radius equal to that at 45° latitude. But this simplification can lead to errors of the order of 1 minute of time. We recommend predictions include proper allowance for oblateness (which is almost trivial in computer-generated predictions).

Further, the Chauvenet '2-percent rule' for computing the enlarged umbral radius, long adopted in the national almanacs of the United Kingdom and United States, leads to an error that is dependent upon the lunar distance. The Danjon method is clearly preferable in this respect.

We consider that predictions of the primary contact times of lunar eclipses, past and future, should be based on a Danjon-like approach with full allowance for an oblate Earth, with the umbral radius r_u being computed using

$$r_u = R_\oplus \pi_{Moon} - s_{Sun} + \pi_{Sun},$$

where

- $R_\oplus = 1 + h - 0.003353 \sin^2 \psi \cos^2 (\delta_{Sun} + f \sin \psi)$,
- $h = 0.0136$ is the adopted height of the notional eclipse-forming layer in Earth radii (corresponding to the mean height derived in this paper, of 87 km),
- ψ is the angular position angle (measured from the east–west direction, positive to the north) of the relevant contact point about the edge of the umbra, and
- $f = s_{Sun} - R_\oplus \pi_{Sun}$.

The calculation requires only a single iteration to generate mutually consistent values of $R_\oplus$ and ψ.

Acknowledgments

We thank the 700+ observers whose observations have been included in the dataset. Without their timings over the last 170 years, this analysis would not have been possible. We are especially indebted to Byron Soulsby (1932–2009) and Joseph Ashbrook (1918–1980), who played a large rôle in collecting and preserving these timings. Before their untimely deaths, both had planned to carry out an analysis like ours.

Addresses: DH: 3, Lupin Place, Murrumbateman, NSW 2582, Australia [DRHerald@bigpond.net.au]
RS: PO Box 126, Norwell, Massachusetts 02061, USA [rsinnott@post.harvard.edu]

References and notes

1 Anon., *Phil.Trans.Roy.Soc.*, **40,** 92–98 (1737)
2 Hire P. de la, *Tabulae Astronomicae*, Paris, 1687. On page 73 he states that 1' 30" is to be added 'propter umbram atmosphærae' (because of the shadow of the atmosphere). Starting with the 1702 edition of the tables, the augmentation was revised to 1' exactly.
3 Houzeau J. C., *Vade-Mecum de l'Astronomie*, Bruxelles, 1882. See pp. 322–324.
4 Donitch N., *Astronomische Nachrichten*, **151,** 3–10 (1899)
5 Chauvenet W., *A Manual of Spherical and Practical Astronomy*, Philadelphia, 1863. See p. 542 of vol. 1.
6 Nautical Almanac Offices (USNO & UK), *Astronomical Almanac for the Year 2014*, Washington & London, 2013. See p. A83.
7 Danjon A., *l'Astronomie*, **65**, 51–53 (1951)
8 Mora E., *l'Astronomie*, **50**, 89–92 (1936)
9 Link F., Ch.. 6, pp. 161–230, in Kopal Z., *Physics and Astronomy of the Moon*, New York & London, 1962
10 Karkoschka E., *Sky Telesc.*, **92**(3), 98–100 (1996 Sept.)
11 Danjon A., *l'Astronomie*, **35,** 261–265 (1921)
12 Bouška J. & Švestka Z., *Bull. Astron. Inst. Czech.*, **2**, 6–7 (1950)
13 Link F. & Linkova Z., *ibid.*, **5**, 82–84 (1954)
14 Belserene E. P., *Sky Telesc.*, **76,** 288–290 (1988 Sept.)
15 Keen R. A., *Science*, **222**, 1011–1013 (1983)
16 Hofmann D. *et al.*, *Geophysical Monograph* **139**, 57–74 (2003)
17 Brooks E., *Sky Telesc.*, **27**, 346–348 (1964 June)
18 Anon., *ibid.*, **27**, 142–146 (1964 March)
19 Ashbrook J., *ibid.*, **27**, 156–160 (1964 March)
20 Ahnert P. & Meeus J., *Die Sterne*, **45**, 116–117 (1969)
21 Kosik S. M., *Bull. Tashkent Astron. Obs.*, **2**, 79 (1940)
22 Bouška J., *Bull. Astron. Inst. Czech.*, **2**(1), 75–76 (1950)
23 Schilling G. F., *J. .Atmosph. Sci.*, **22**, 110–115 (1965)
24 Soulsby B., *J. Brit. Astron. Assoc.*, **95**(1), 16–21 (1984)
25 Soulsby B., *Austr. J. Astron.*, **3**(4), 156–162 (1990)
26 Soulsby B., *J. Brit. Astron. Assoc.*, **100**, 293–305 (1990)
27 Soulsby B., *Proc. Astron. Soc. Austr.*, **10**(2), 131–133 (1992)
28 Bouška J., *Bull. Astron. Inst. Czech.*, **9**(6), 245–247 (1958)
29 Bouška J., *ibid.*, **11**, 145–148 (1960)
30 Marmet P. & Couture C., 'Enlargement of the Earth's Shadow on the Moon: An Optical Illusion'. Retrieved in 2013 from **http://www.newtonphysics.on.ca/astronomy/index.html**

Received 2013 October 20; accepted 2014 January 29